Bounded UDE-Based Controller for Input Constrained Systems With Uncertainties and Disturbances

Yeqin Wang, *Member, IEEE*, Beibei Ren, *Senior Member, IEEE*, and Qing-Chang Zhong, *Fellow, IEEE*

***Abstract*—The uncertainty and disturbance estimator (UDE)-based controller has emerged as an effective robust control method to handle systems with uncertainties and disturbances. However, similar to other controllers including an integral action, the UDE-based controller faces the integral windup issue when the system has input constraints. In this article, a bounded UDE-based controller is proposed to deal with systems subject to uncertainties, disturbances, and input constraint. An additional time-varying variable is introduced into the design of the error dynamics to naturally avoid integral windup. The boundedness design guarantees that both the final controller output and the additional time-varying variable dynamically move on an ellipse so that the controller output always satisfies the input constraint. The proposed bounded UDE-based controller inherits the robustness of the conventional UDE-based control method, and has a clear structure, with guidelines provided for parameter selections. Both theoretical analysis and experimental results are provided to validate the proposed design.**

***Index Terms*—Boundedness design, input constraint, integral windup, uncertainty and disturbance estimator (UDE).**

I. Introduction

UNCERTAINTIES and disturbances are common issues faced by control system design. A robust control method, referred to the uncertainty and disturbance estimator (UDE)-based controller [1], was proposed to handle uncertainties and disturbances for linear time-invariant (LTI) systems as a replacement of the time-delay controller (TDC) [2]. Compared to the TDC, the UDE-based controller [1] does not need to measure the derivative of the states, and no oscillations exist in the control signal. In the UDE-based control design, a filter is adopted to estimate and compensate uncertainties and disturbances. As a result, the challenging problem of designing a robust controller is converted into the design of the filter. In recent years, the UDE-based controller demonstrated excellent performances in broad practical applications in both linear and nonlinear systems, e.g., variable-speed wind turbine control [3], solar system control [4], motor drives [5], power electronics control [6], [7], quadrotors [8], a class of nonminimum phase systems [9], robot manipulator tracking [10], robust input–output linearization [11], etc. The idea of the UDE was also further extended to the sliding-mode control [12] to improve the robustness. A two-degree-of-freedom nature of the UDE-based controller was disclosed in [13]. A rough first-order plus time-delay (FOPDT) model was introduced into the UDE-based controller to handle apparent lag and time delay [14]. The asymptotic reference tracking and disturbance rejection of the UDE-based controller were achieved in [15] based on the internal model principle (IMP). The tradeoff between the tracking and disturbance rejection under finite bandwidth constraints in the UDE-based controller was investigated in [16]. The phase margin constraint of actuator dynamics was investigated for the design of the UDE-based controller in [17].

The constraint of the system input is another common problem in practice, due to the physical limitation of the actuators or the safety requirement of the operations. The constraint of the system input results in a difference between the actual plant input and the controller output, when a large control effort is required. The controller output cannot drive the plant properly, while it continually increases during the integral action of the none-zero state tracking error in this scenario. This phenomenon is named "integral windup" or "integrator windup" [18], which usually leads to the performance deterioration or even the instability of the control system [19], [20]. The UDE-based controller faces the same challenge. It is not an easy task to consider the input constraint for the UDE-based controller, as it includes the integral terms to eliminate the tracking error. A common method to handle integral windup is through linear or nonlinear anti-windup designs [20], but this still cannot guarantee system stability in the original form or requires additional knowledge of

Manuscript received May 3, 2019; revised August 23, 2019 and December 8, 2019; accepted December 30, 2019. Date of publication January 29, 2020; date of current version October 30, 2020. *(Corresponding author: Beibei Ren.)*

Y. Wang was with the National Wind Institute, Texas Tech University, Lubbock, TX 79409-1021 USA. He is now with the Syndem LLC, Chicago, IL 60616 USA (e-mail: yeqin.wang@ttu.edu).

B. Ren is with the Department of Mechanical Engineering, Texas Tech University, Lubbock, TX 79409-1021 USA (e-mail: beibei.ren@ttu.edu).

Q.-C. Zhong is with the Department of Electrical and Computer Engineering, Illinois Institute of Technology, Chicago, IL 60616 USA (e-mail: zhongqc@ieee.org).

Color versions of one or more of the figures in this article are available online at https://ieeexplore.ieee.org.

Digital Object Identifier 10.1109/TIE.2020.2969069

the system structure and parameters [19]. Recently, a bounded integral controller (BIC) has been proposed in [19] to handle input constraint with the improvement of the conventional integral control, which automatically guarantees the boundedness of the controller output without any switches. Though the BIC can handle both input constraint and integral windup simultaneously, its robust performance is limited by the single integral action. Moreover, the BIC requires the system to be bounded-input bounded-output (BIBO) stable. It is worth noting that the input constraint is also considered as a part of the optimal control problem [21]. However, these kinds of designs usually require large computational efforts, which might not be preferred for real-time control systems that require fast response [22].

Motivated by the BIC [19], a boundedness design is proposed in this article for the UDE-based controller to deal with input constraint, uncertainties, and disturbances without integral windup. The contributions of this article are highlighted as follows:

1) An ellipse is designed to make the system input (the final controller output) always move and remain on the ellipse to satisfy the input constraint.
2) When the final controller output u approaches its bounds, the additional time-varying variable in the new error dynamics will approach 0, which mitigates the continuous effect of the integral action on the tracking error and avoids the integral windup.
3) A dynamic controller with the boundedness design is developed for both the final controller output and the time-varying variable to achieve the ellipse design, where the input of the dynamic controller is the output of the newly modified UDE-based control law to handle uncertainties and disturbances.
4) Boundedness analysis, parameter analysis, stability analysis, performance analysis, and experimental results are provided to validate the proposed design.

Compared to the existing anti-windup designs using the auxiliary systems in [23], the proposed boundedness design is embedded into the conventional UDE structure, and the whole controller becomes a bounded UDE-based controller. This bounded UDE-based controller inherits the robustness of the conventional UDE method, and has a clear structure with guidelines provided for parameter selections. Moreover, the BIBO assumption in [19] is relaxed. Compared with our preliminary results [24] for the symmetric constraint with respect to the origin, in this work, the regular interval constraint for controller outputs are considered, which is more general in real applications, e.g., battery voltage or other nonnegative dc voltage, engine torque, etc. The midpoint of the constrained interval is selected to facilitate both boundedness design and Lyapunov analysis. The scenario considered in [24] is a special case of this work. The insights of key parameters are revealed, and more rigorous stability analysis is given. Furthermore, extensive experimental results for speed control of a dc motor–generator coupled system are provided to validate the effectiveness of the proposed control, including comparisons with both the conventional UDE-based control (6) in [1] plus a saturation unit and the BIC in [19], and guidelines for selecting key parameters.

II. Overview of UDE-Based Controller and Problem Formulation

A. The UDE-Based Controller

Consider a class of single-input LTI systems

$$\dot{x} = Ax + f(x) + Bu + d(t) \tag{1}$$

where $x = [x_1, x_2, \ldots, x_n]^T \in R^n$ is the system state, $u \in R$ is the system input, $A \in R^{n\times n}$ is the known system matrix, $B \in R^n$ is the known control vector, $f(x) \in R^n$ is the unknown linear or nonlinear system dynamics, and $d(t) \in R^n$ is the bounded external disturbance. A stable reference model is selected according to the desired performance as

$$\dot{x}_m = A_m x_m + B_m c(t) \tag{2}$$

where $x_m \in R^n$ is the reference state vector, and $c(t) = [c_1, c_2, \ldots, c_r]^T \in R^r$ is a piecewise continuous and uniformly bounded command for the reference model, $A_m \in R^{n\times n}$ and $B_m \in R^{n\times r}$.

The objective is to design a control law u such that the state x can asymptotically track its reference x_m, where the tracking error $e_x = x_m - x$ satisfies the error dynamics

$$\dot{e}_x = (A_m + K)e_x \tag{3}$$

where $K \in R^{n\times n}$ is a constant matrix, and the error feedback gain matrix $(A_m + K)$ should be Hurwitz.

With the requirements above, the control law u is designed as

$$Bu = A_m x_m + B_m c(t) - Ax - u_d - (A_m + K)e_x \tag{4}$$

where the lumped term $u_d = f(x) + d(t)$ consists of the unknown term $f(x)$ and the disturbance $d(t)$.

Following the UDE procedures in [1], u_d can be approximated as

$$\begin{aligned}\hat{u}_d &= L^{-1}\{G_f(s)\} * u_d \\ &= L^{-1}\{G_f(s)\} * (\dot{x} - Ax - Bu)\end{aligned}$$

where $*$ is the convolution operator and $G_f(s)$ is the UDE filter with both strictly proper stable manner and appropriate bandwidth to cover the spectrum of u_d. L^{-1} means inverse Laplace transformation. Replacing u_d with $\hat{u}_d$ in (4), there is

$$\begin{aligned}Bu = {} & A_m x_m + B_m c(t) - Ax - (A_m + K)e_x \\ & - L^{-1}\{G_f(s)\} * (\dot{x} - Ax - Bu).\end{aligned} \tag{5}$$

Then, the original UDE-based control law is formulated as

$$\begin{aligned}u = B^+ \Bigg[& -Ax + L^{-1}\left\{\frac{1}{1 - G_f(s)}\right\} \\ & * [A_m x_m + B_m c(t) - (A_m + K)e_x] \\ & - L^{-1}\left\{\frac{sG_f(s)}{1 - G_f(s)}\right\} * x\Bigg]\end{aligned} \tag{6}$$

where $B^+ = (B^T B)^{-1} B^T$. Equation (6) is the accurate solution of (5) if the following structural constraint [15] is met:

$$\begin{aligned}(I - BB^+) \cdot [& A_m x_m + B_m c(t) - Ax \\ & - (A_m + K)e_x - \hat{u}_d] = 0.\end{aligned}$$

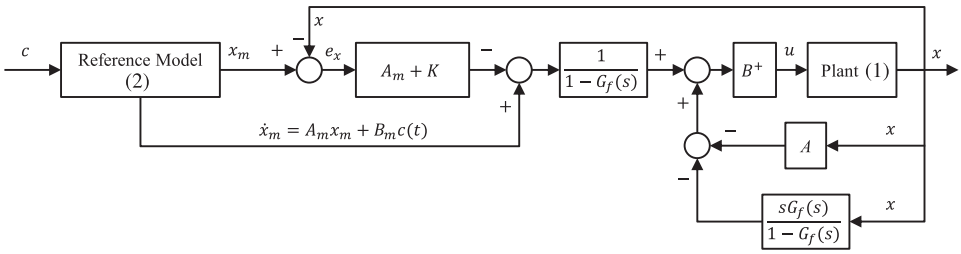

Fig. 1. Scheme of the conventional UDE-based controller in [1].

TABLE I
EXAMPLES OF THE FILTER DESIGN AND INTEGRAL ACTION IN THE UDE-BASED CONTROLLER (6)

G_f	$\frac{1}{1-G_f(s)}$	$\frac{sG_f(s)}{1-G_f(s)}$
$G_{f1}(s) = \frac{a_0}{s+a_0}$	$1 + \frac{a_0}{s}$	a_0
$G_{f2}(s) = \frac{a_0}{s^2+a_1 s+a_0}$	$1 + \frac{1}{s} \cdot \frac{a_0}{s+a_1}$	$\frac{a_0}{s+a_1}$
$G_{f3}(s) = 1 - \frac{s(s^2+\omega_0^2)}{(s+a_0)(s^2+a_1 s+\omega_0^2)}$	$1 + \frac{a_0}{s} + \frac{a_1(s+a_0)}{s^2+\omega_0^2}$	$a_0 + a_1 + \frac{a_1(a_0 s-\omega_0^2)}{s^2+\omega_0^2}$

Otherwise, it is the least-squares approximate solution of (5). The scheme of the UDE-based controller with the two-degree-of-freedom [13] is shown in Fig. 1.

B. Integral Action in the UDE-Based Controller

In the UDE-based controller (6), there are two terms involving the filter, $\frac{1}{1-G_f(s)}$ and $\frac{sG_f(s)}{1-G_f(s)}$. The filter design plays a very important role to estimate the uncertainties and disturbances and to achieve good control performance [13], [15]. Theoretically, if the filter is chosen as a strictly proper stable filter with unity gain and zero phase shift over the spectrum of the uncertainties and disturbances, the asymptotic reference tracking and disturbance rejection can be achieved [13], [15], and the systematical filter design has been provided in [15] based on the IMP [25]. If both of the reference and the lumped uncertain term are step signals, the low-pass filter with $G_f(0) = 1$ is enough to serve the purpose. If the lumped uncertain term includes sinusoidal signals, one or multiple second-order bandpass filters can be combined in the filter design to handle the disturbances with one or multiple frequency components. Table I lists three commonly used UDE filters. $G_{f1}(s)$ in [1], [3], [4] and $G_{f2}(s)$ in [26] are commonly used first-order and second-order low-pass filters, because they can be easily implemented. G_{f3} in [15], [27] is the combination of a first-order low-pass filter and a second-order bandpass filter to handle the lumped uncertain term consisting of both step and sinusoidal signals. It is interesting to note that the integral action always appears in the $\frac{1}{1-G_f(s)}$ term for the three different filters, and the $\frac{sG_f(s)}{1-G_f(s)}$ term does not include the integral action due to the s term in the numerator. The integral action in the $\frac{1}{1-G_f(s)}$ term is caused by the property of the low-pass filter.

While the integral action in $\frac{1}{1-G_f(s)}$ acting on the tracking error in (6) is important to achieve good steady-state tracking performance, specially for both step reference and step disturbances, it might cause integral windup if the system input is subject to a constraint. The anti-windup designs in [20] are commonly adopted to deal with this issue; however, the information of system structure and parameters is usually required to guarantee the closed-loop system stability [19]. Furthermore, anti-windup designs with auxiliary systems [20], [23] will become very complex with the increasing number of design parameters, if the system order increases. Usually, it is difficult to have clear guidelines to select design parameters for anti-windup designs. As for BIC in [19], it requires the BIBO stability of the original systems. Is it possible to have a boundedness design for the UDE-based controller to handle the integral windup and to guarantee the closed-loop system stability simultaneously?

Note that the integral action in the $\frac{1}{1-G_f(s)}$ term also acts on the reference model $\dot{x}_m = A_m x_m + B_m c(t)$, as shown in Fig. 1. In this work, $c(t)$ is assumed to be uniformly bounded, then x_m can converge to a bounded value through the proper stable reference model design. Therefore, the reference model part does not have the integral windup issue.

C. Problem Formulation

Considering system (1) and the system input subject to an interval constraint

$$u \in (u_{\min},\ u_{\max}) \tag{7}$$

where $u_{\min}$ and $u_{\max}$ are constant bounds with $u_{\max} > u_{\min}$; the control objective is to design a robust control law u such that the state x can asymptotically track its reference x_m in (2), while the integral windup issue, uncertainties, and disturbances can be handled simultaneously. The bounds $u_{\min}$ and $u_{\max}$ are usually determined according to the physical limitation of the actuators or the safety requirement of the operations.

III. BOUNDED UDE-BASED CONTROLLER

In this section, a boundedness design is proposed for the conventional UDE-based controller to handle input constraint, uncertainties, and disturbances without integral windup. Unlike

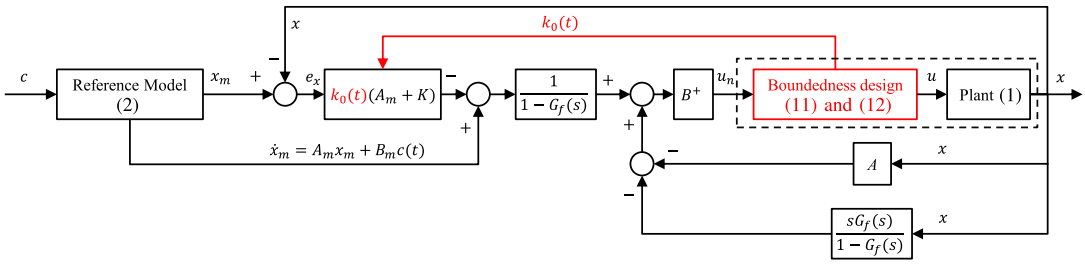

Fig. 2. Scheme of the proposed bounded UDE-based controller.

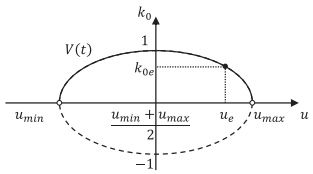

Fig. 3. An illustration of the bounded controller output u and the additional variable k_0 with the proposed bounded UDE-based controller (10)–(12).

the auxiliary system design, this boundedness design is embedded into the conventional UDE structure to result in a bounded UDE-based controller, as shown in Fig. 2. The stability analysis and the performance analysis of the closed-loop system are provided.

A. Control Design

In the conventional UDE-based controller (6), the integral windup is caused by the integral action in $\frac{1}{1-G_f(s)}$ acting on the tracking error continuously, when the system input is constrained. First, in order to mitigate the continuous effect of the integral action on the tracking error, an additional time-varying variable $0 < k_0(t) \leq 1$ is introduced into the original error dynamics (3) as follows:

$$\dot{e}_x = k_0(t)(A_m + K)e_x. \tag{8}$$

If k_0 can approach 0 when the final controller output u approaches its bounds in (7), the integral windup can be avoided. The requirements of both input constraint in (7) and time-varying variable k_0 can be achieved if the system input or the final controller output u and the time-varying variable k_0 can always move and remain on an ellipse shown in Fig. 3, which can be described as

$$\frac{4\left(u - \frac{u_{\max}+u_{\min}}{2}\right)^2}{(u_{\max}-u_{\min})^2} + k_0^2 = 1. \tag{9}$$

Second, based on the new error dynamics (8) and the UDE design procedures in Section II, the UDE-based control law is modified as

$$\begin{aligned} u_n = B^+\Bigg[&- Ax + L^{-1}\left\{\frac{1}{1-G_f(s)}\right\} \\ &* [A_m x_m + B_m c(t) - k_0(A_m+K)e_x] \\ &- L^{-1}\left\{\frac{sG_f(s)}{1-G_f(s)}\right\} * x\Bigg]. \end{aligned} \tag{10}$$

Third, in order to achieve the desired ellipse in (9), a dynamic controller with boundedness design is developed for the final controller output u and the time-varying variable k_0 with u_n in (10) as the input

$$\begin{aligned} \dot{u} = &- k_1\left(u - \frac{u_{\max}+u_{\min}}{2}\right) \\ &\cdot\left(\frac{4\left(u - \frac{u_{\max}+u_{\min}}{2}\right)^2}{(u_{\max}-u_{\min})^2} + k_0^2 - 1\right) \\ &- k_2 k_0^2 (u - u_n) \end{aligned} \tag{11}$$

$$\begin{aligned} \dot{k}_0 = &- k_1 k_0\left(\frac{4\left(u - \frac{u_{\max}+u_{\min}}{2}\right)^2}{(u_{\max}-u_{\min})^2} + k_0^2 - 1\right) \\ &+ \frac{4k_2\left(u - \frac{u_{\max}+u_{\min}}{2}\right)}{(u_{\max}-u_{\min})^2} k_0 (u - u_n) \end{aligned} \tag{12}$$

where u is the final controller output, $\frac{u_{\max}+u_{\min}}{2}$ is the midpoint of the constrained interval, k_1 and k_2 are positive constants, and k_0 is the additional design variable fed into the new error dynamics (8). The boundedness design (11) and (12) are not affected by the system order in system (1) and do not cost much computational resources. Guidelines on the implementation of (11) and (12) are provided in the Appendix.

Furthermore, the boundedness of the proposed design (11) and (12) is analyzed through the following Lemma.

Lemma 1: Through the boundedness design (11) and (12), the final controller output u and the time-varying variable k_0 are regulated within the ellipse (9), and u is kept within the given range of $(u_{\min},\ u_{\max})$.

Proof: Consider the following Lyapunov function candidate:

$$V(t) = \frac{4\left(u - \frac{u_{\max}+u_{\min}}{2}\right)^2}{(u_{\max}-u_{\min})^2} + k_0^2. \tag{13}$$

Taking the derivative of $V(t)$ along (11) and (12), it yields

$$\dot{V}(t) = -2k_1 V^2(t) + 2k_1 V(t). \tag{14}$$

Then, solving (14) gives

$$V(t) = \frac{1}{1 - e^{-2k_1 t}\left(1 - \frac{1}{V(0)}\right)}. \tag{15}$$

Through the initial design of $V(0) = 1$, e.g., with $k_0(0) = 1$, and $u(0) = \frac{u_{\max}+u_{\min}}{2}$, then

$$V(t) = 1 \quad \forall t \geq 0.$$

According to (13), it always holds that $\frac{4(u-\frac{u_{\max}+u_{\min}}{2})^2}{(u_{\max}-u_{\min})^2}+k_0^2=1$. So, u is kept within the given range of $(u_{\min},\ u_{\max})$. This completes the proof. ■

With the proposed boundedness design, u and k_0 will start and always remain on the ellipse (9), no matter how u_n in (10) changes, as shown in Fig. 3. At the steady state, $\dot{u}$ and $\dot{k}_0$ will be regulated to 0 with the zero tracking error of the system state x. When $\dot{u}=0$ and $\dot{k}_0=0$, both controller states u and k_0 will converge to an equilibrium point $(u_e,\ k_{0e})$. The scheme of the proposed boundedness design for the UDE-based controller is shown in Fig. 2. Compared to the conventional UDE-based controller in Fig. 1, the boundedness design is well embedded into the UDE-based control framework with a clear structure and the whole controller becomes a bounded UDE-based controller. Compared with the preliminary results in [24], the midpoint of the constrained interval is introduced in both boundedness design and Lyapunov analysis, which works for more general interval input constraint.

B. Insights of the Parameters

Similar to the conventional UDE-based controller, the error dynamics (8) and the filter design still play an important role in the bounded UDE-based controller. It is worth noting that the time-varying variable k_0 decreases when the final controller output u moves toward its bounds, as shown in Fig. 3. This will degrade the control performance of the bounded UDE-based controller to some extent, especially the transient performance, compared to the conventional UDE-based controller with the same control parameters. This effect can be mitigated by choosing (A_m+K) to have fast transient responses. Similar to the discussions in Section II-B about the filter design, the filter bandwidth should cover all the spectrum of the uncertainties and disturbances to achieve good control performance, even when the plant includes fast-varying uncertainties or disturbances.

In the bounded UDE-based controller (10)–(12), three new parameters k_1, k_2, and k_0 are introduced. According to (15), if there are any numerical errors or parameter drifts in $V(t)$, $V(t)$ will still converge to 1 through the exponential term of k_1 as $t\to\infty$, and the rate of convergence can be adjusted by the parameter k_1.

When $V(t)=1$, i.e., when the controller operates on the ellipse, the boundedness design (11) and (12) are reduced to

$$\dot{u}=-k_2k_0^2(u-u_n) \tag{16}$$

$$\dot{k}_0=\frac{4\left(u-\frac{u_{\max}+u_{\min}}{2}\right)}{(u_{\max}-u_{\min})^2}k_2k_0(u-u_n). \tag{17}$$

When the final controller output u is not close to its bounds and k_0 is not close to 0, u will converge to u_n, and the rate of convergence can be adjusted by the parameter k_2. If u is not equal to u_n, the nonzero $\dot{u}$ will drive u to u_n. In order to handle fast-varying uncertainties or disturbances, the parameter k_2 should be big enough to cover the effective bandwidth of the modified controller output u_n. Theoretically, k_2 can be designed as a very large number. In practice, the selection of k_2 should consider the sampling frequency of the digital controller when realizing the discrete implementation of (16). For example, (16) can be discretized with the forward-difference method as

$$\frac{u(k+1)-u(k)}{T}=-k_2k_0^2(k)[u(k)-u_n(k)]$$

then,

$$u(k+1)=\left[1-Tk_2k_0^2(k)\right]u(k)+k_2k_0^2(k)u_n(k) \tag{18}$$

where k is the sample index and T is the sampling period of the digital controller. In order to ensure the stability of the discrete equation (18), k_2 should be selected to fulfill

$$-1<1-k_2k_0^2(k)T<1.$$

In order to further avoid the control signal ringing, $1-k_2k_0^2(k)T\geq 0$ is required. Therefore, k_2 needs to satisfy

$$0<k_2\leq\min\left(\frac{1}{k_0^2(k)T}\right)=\frac{1}{T}.$$

More information about discrete implementation can be founded in [28]–[30].

When u is close to its bounds, the variable k_0 will converge to 0. Then, the term $L^{-1}\{\frac{1}{1-G_f(s)}\}*[k_0(A_m+K)e_x]$ in (10) will converge to zero as $k_0\to 0$. This means that the integral action in (10) slows down and converges to zero, when u goes to its bounds, which can naturally prevent integral windup. In other words, u_n will converge to a bounded value, when u moves to its bounds. According to (16) and (17), the interesting part of the boundedness design is that $\dot{u}$ and $\dot{k}_0$ also converge to 0, when k_0 converges to 0. When u_n violates the bounds, u will converge to its bounds and k_0 will converge to 0. However, k_0 will not reach 0, because the convergence rate $\dot{k}_0$ gradually converges to 0 as well. The detailed analysis can be found in [19]. Through the initial design, e.g., with $k_0(0)=1$, and $u(0)=\frac{u_{\max}+u_{\min}}{2}$, k_0 will remain on the upper half-plane of the ellipse, as shown in Fig. 3. Therefore, $0<k_0\leq 1$ can hold for the proposed design.

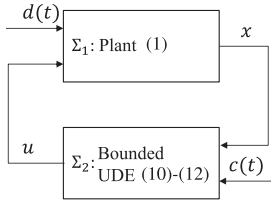

Fig. 4. The closed-loop system with the composite interconnection form.

C. Stability Analysis

In this article, the bounded UDE-based controller is proposed to handle the uncertainties and disturbances, and input constraint without integral windup. Integral windup issue usually happens to system (1) with input-to-state (practical) stability (ISpS) property. The stability analysis for system (1) with ISpS property will be discussed first. By applying the bounded UDE-based controller (10)–(12) to plant (1), the closed-loop system is formed as a composite interconnection form, as shown in Fig. 4.

Theorem 2: The closed-loop system shown in Fig. 4 is ISpS, if plant (1) is ISpS.

Proof: Based on Lemma 1 and the small-gain theorem in [31], it can be proven that the closed-loop system in Fig. 4 is ISpS. Due to page limit, the proof is omitted. A similar proof can be found in [19]. ■

If system (1) is not ISpS, it is required that system input within the range $u \in (u_{\min},\ u_{\max})$ is capable to stabilize the system. When u converges to the bounds, particularly for a period, the closed-loop system usually becomes unstable. Though the integral windup still can be handled by the proposed design, the closed-loop system usually cannot be stabilized, if the system is not controllable. The proposed bounded UDE-based controller also can be applied to general LTI systems, which do not satisfy the ISpS property but should be controllable. The related discussions are given below. As shown in Fig. 2, the boundedness design (11) and (12) and plant (1) can be combined together and regarded as a new plant (inside the dashed box) with the system input u_n (10), where both x and k_0 are system states. Then, the boundedness design can be treated as a disturbance $\Delta \in R^n$ for the new plant as

$$\dot{x} = Ax + f(x) + Bu_n + d(t) + \Delta \tag{19}$$

where $\Delta = B(u - u_n)$. And the lumped term becomes $u_d = f(x) + d(t) + \Delta$.

Corollary 3: Consider the closed-loop system shown in Fig. 2. Given any compact set $\Omega_x = \{x \mid \|x\|^2 < q,\ q > 0\}$, the closed-loop system is stable in the sense of boundedness if the following conditions are met:

1) the initial state $x(0)$ is within this set Ω_x;
2) $f(x)$ satisfies the Lipschitz condition
$$\|f(x)\| \le F\|x\| + D \tag{20}$$
where $\|\cdot\|$ denotes the Euclidean norm with F and D being positive constants;
3) system (1) is controllable for the input within the range $u \in (u_{\min},\ u_{\max})$;
4) the following structural constraint is met:
$$\left(I - BB^{+}\right) \cdot \left[A_m x_m + B_m c(t) - Ax - k_0(A_m + K)e_x - \hat{u}_d\right] = 0; \tag{21}$$
5) there exist real positive definite matrices P and Q such that
$$Q = -\frac{(A_m + K)^T P + P(A_m + K)}{\|P\|} \tag{22}$$
with the minimal eigenvalue of Q satisfying
$$\lambda_{\min}(Q) > \frac{2F + \varepsilon_2^2 + \frac{\lambda_{\max}(P)}{q\lambda_{\min}(P)}\left(\frac{\max_t(k_0)\|x_m\|}{\varepsilon_1^2} + \frac{p^2}{\varepsilon_2^2}\right)}{\min_t(k_0)} + \varepsilon_1^2\|x_m\|\|K\|^2 \tag{23}$$
with $\varepsilon_1 > 0$ and $\varepsilon_2 > 0$ being tuning parameters, $p > 0$ as the upper bound of the variable $\zeta = (1 - k_0)\|A_m\|\|x_m\| + \|B_m c\| + \|d\| + \|\Delta\| + D$, and $\lambda_{\max}(P)$ and $\lambda_{\min}(P)$ as the maximum and minimum eigenvalues of P, respectively.

Proof: According to Theorem 4.6 in [32], given any real symmetric positive definite matrix Q_0, there exists a real symmetric positive definite matrix P to satisfy

$$(A_m + K)^T P + P(A_m + K) = -Q_0.$$

Let $Q = \frac{Q_0}{\|P\|}$, there exist real positive definite matrices P and Q such that (22) holds.

Consider the following Lyapunov function candidate:

$$V_x(x) = x^T P x.$$

Taking the derivative of $V_x(x)$ along with the new plant (19) and the modified UDE-based control law (10), there is

$$\begin{aligned}
\dot{V}_x(x) &= \dot{x}^T P x + x^T P \dot{x} \\
&= k_0 x^T \left[(A_m + K)^T P + P(A_m + K)\right] x \\
&\quad + (1 - k_0)\left(x_m^T A_m^T P x + x^T P A_m x_m\right) \\
&\quad - k_0\left(x_m^T K^T P x + x^T P K x_m\right) \\
&\quad + c^T B_m^T P x + x^T P B_m c \\
&\quad + L^{-1}\{1 - G_f(s)\} * \left[f^T(x) P x + x^T P f(x)\right] \\
&\quad + L^{-1}\{1 - G_f(s)\} \\
&\quad * \left[\left(d^T + \Delta^T\right) P x + x^T P (d + \Delta)\right] \\
&\le -k_0\lambda_{\min}(Q)\|P\|\|x\|^2 \\
&\quad + 2(1 - k_0)\|A_m\|\|P\|\|x_m\|\|x\| \\
&\quad + 2k_0\|K\|\|P\|\|x_m\|\|x\| + 2\|B_m c\|\|P\|\|x\| \\
&\quad + L^{-1}\{1 - G_f(s)\} * \left(2F\|P\|\|x\|^2\right) \\
&\quad + L^{-1}\{1 - G_f(s)\} * [2(\|d\| + \|\Delta\| + D)\|P\|\|x\|] \\
&\le \left[-k_0\lambda_{\min}(Q)\|P\| + 2F\|P\|\right]\|x\|^2 \\
&\quad + 2k_0\|x_m\|\|K\|\|x\|\|P\| + 2\zeta\|x\|\|P\|
\end{aligned} \tag{24}$$

where $\zeta = (1 - k_0)\|A_m\|\|x_m\| + \|B_m c\| + \|d\| + \|\Delta\| + D$. By applying the Young's inequality to (24), there is

$$\begin{aligned}
\dot{V}_x(x) &\le -\left[k_0\lambda_{\min}(Q) - \varepsilon_1^2 k_0\|x_m\|\|K\|^2 - 2F - \varepsilon_2^2\right] \cdot \|P\|\|x\|^2 + \frac{k_0\|x_m\|\|P\|}{\varepsilon_1^2} + \frac{\zeta^2\|P\|}{\varepsilon_2^2} \\
&= -\frac{\left[k_0\lambda_{\min}(Q) - \varepsilon_1^2 k_0\|x_m\|\|K\|^2 - 2F - \varepsilon_2^2\right]}{\lambda_{\max}(P)} \cdot \lambda_{\max}(P)\|x\|^2\|P\| + \left(\frac{k_0\|x_m\|}{\varepsilon_1^2} + \frac{\zeta^2}{\varepsilon_2^2}\right)\|P\| \\
&\le \left[-\lambda_1 V_x(x) + \lambda_2\right]\|P\|
\end{aligned} \tag{25}$$

where $\lambda_1 = \left[\frac{\min_t(k_0)[\lambda_{\min}(Q) - \varepsilon_1^2\|x_m\|\|K\|^2] - 2F - \varepsilon_2^2}{\lambda_{\max}(P)}\right]$, $\lambda_2 = \frac{\max_t(k_0)\|x_m\|}{\varepsilon_1^2} + \frac{p^2}{\varepsilon_2^2}$, $\varepsilon_1 > 0$ and $\varepsilon_2 > 0$ are tuning parameters to

determine the value of λ_2, and can be selected to minimize the right-hand side of inequality (23). From condition (23), there is

$$\lambda_{\min}(P)q > \frac{\lambda_2}{\lambda_1}.$$

Therefore, $\dot{V}_x(x) < 0$, when $V_x(x) \geq \lambda_{\min}(P)q > \frac{\lambda_2}{\lambda_1}$. This indicates $V_x(x) \leq \lambda_{\min}(P)q$, then, $\|x\|^2 \leq q$ for all $t > 0$ if $\|x(0)\|^2 \leq q$. So, the set Ω_x is an invariant set. The closed-loop system is stable in the sense of boundedness. ■

D. Performance Analysis

For the new plant (19) and the modified UDE-based control law (10), as illustrated in Fig. 2, the state tracking performance will be analyzed.

When the UDE filter is used to estimate the uncertain term u_d, u_d is replaced with $\hat{u}_d$ for the modified UDE-based control law (10). Since the structural constraint (21) is met, different from (8), the actual error dynamics becomes

$$\dot{e}_x = k_0(A_m + K)e_x - \tilde{u}_d \tag{26}$$

where $\tilde{u}_d \triangleq u_d - \hat{u}_d$ is the estimation error of the lumped term $u_d = f(x) + d(t) + \Delta$, and can be calculated as

$$\tilde{u}_d = L^{-1}\{1 - G_f(s)\} * u_d. \tag{27}$$

Consider the following Lyapunov function candidate:

$$V_e(e_x) = e_x^T P e_x.$$

Then,

$$\begin{aligned}\dot{V}_e(e_x) &= k_0 e_x^T Q e_x \|P\| - \tilde{u}_d^T P e_x - e_x^T P \tilde{u}_d \\ &\leq -k_0 \lambda_{\min}(Q)\|P\|\|e_x\|^2 + 2\|\tilde{u}_d\|\|e_x\|\|P\| \\ &\leq \frac{\left[-k_0\lambda_{\min}(Q) + \varepsilon_3^2\right]\|P\|\lambda_{\max}(P)\|e_x\|^2}{\lambda_{\max}(P)} \\ &\quad + \frac{\|\tilde{u}_d\|^2\|P\|}{\varepsilon_3^2} \\ &\leq -\lambda_3 V_e(e_x) + \lambda_4 \end{aligned} \tag{28}$$

where $\lambda_3 = \frac{[\min_t(k_0)\lambda_{\min}(Q) - \varepsilon_3^2]\|P\|}{\lambda_{\max}(P)}$, $\lambda_4 = \frac{\max_t(\|\tilde{u}_d\|^2)\|P\|}{\varepsilon_3^2} > 0$, and $\varepsilon_3 > 0$ is a tuning parameter. Then, solving (28) gives

$$0 \leq V_e(e_x) \leq V_e(e_x(0))e^{-\lambda_3 t} + \frac{\lambda_4}{\lambda_3}(1 - e^{-\lambda_3 t}). \tag{29}$$

It is easy to achieve $\lambda_3 > 0$, according to Section III-C, if k_0 is not close to 0. The term $V_e(e_x(0))e^{-\lambda_3 t}$ will gradually decay and converge to zero, and the term $\frac{\lambda_4}{\lambda_3}(1 - e^{-\lambda_3 t})$ will gradually increase and converge to $\frac{\lambda_4}{\lambda_3} = \frac{\max_t(\|\tilde{u}_d\|^2)\lambda_{\max}(P)}{\varepsilon_3^2[\min_t(k_0)\lambda_{\min}(Q) - \varepsilon_3^2]}$, when $t \to \infty$. This indicates $V_e(e_x)$ will finally converge to $\frac{\lambda_4}{\lambda_3}$. Through the design of the error feedback gain matrix $(A_m + K)$ in (8), $\lambda_{\min}(Q)$ can be tuned to reduce $\frac{\lambda_4}{\lambda_3}$, according to (22), where the parameter ε_3 can be selected as $\varepsilon_3^2 = \frac{\min_t(k_0)\lambda_{\min}(Q)}{2}$. Then, the tracking error e_x can be reduced as well with $\|e_x\| \leq \sqrt{\frac{V_e(e_x)}{\lambda_{\min}(P)}}$. If the filter $G_f(s)$ is well designed as a strictly proper stable filter with unity gain and appropriate bandwidth to cover all the spectrum of the lumped term u_d, as discussed in Section II-B, the estimation error (27) will be close to zero, so as λ_4. Therefore, $V_e(e_x)$ will converge to zero. Also, with $\|e_x\| \leq \sqrt{\frac{V_e(e_x)}{\lambda_{\min}(P)}}$, the tracking error e_x will converge to zero.

Note that the steady-state performances cannot be guaranteed if k_0 converges to 0, even though the closed-loop system is stable given the ISpS of plant (1).

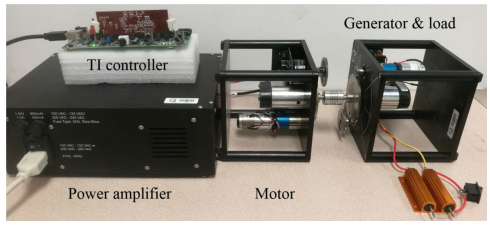

Fig. 5. Experimental test rig.

TABLE II
SYSTEM PARAMETERS OF TEST RIG

Parameters	Values	Parameters	Values
J_m	2.3×10^{-6} kg·m^2	R_m	2.7Ω
k_t, k_ω	7.8×10^{-3} V/(rad/s)	L_m	0.18 mH
b	9.18×10^{-6} Nm/(rad/s)	-	-

IV. EXPERIMENTAL VALIDATION

In order to verify the proposed bounded UDE-based controller, the speed control for a dc motor–generator coupled system is investigated, as shown in Fig. 5. Both the motor and the generator are Quanser rotary servo units. The motor is powered by a Quanser power amplifier. The system input for the power amplifier is from the digital-to-analog converter (DAC) of a Texas Instruments (TI) Peripheral Explorer Kit. The motor speed is measured through an encoder embedded in the servo unit. The generator connected to two 1 Ω resistors with serial connection is performed as a load for the motor. One resistor is bypassed with a switch for load change. The proposed bounded UDE-based controller is implemented in a TI TMS320F28335 microcontroller with 20 kHz sampling frequency. The equivalent dynamic equation of the dc motor can be represented as

$$J_m\dot{\omega} = k_t i - b\omega - T_l \tag{30}$$

$$L_m\dot{i} = u - R_m i - k_\omega\omega \tag{31}$$

where J_m is the equivalent total rotor moment of inertia, ω is the motor speed, $k_t = k_\omega$ is the torque constant or voltage constant, b is the total viscus damping, T_l is the unknown load from the generator side, L_m is the armature inductance, R_m is the armature resistance, and u is the voltage input. In this system, the actuator is the TI Peripheral Explorer Kit plus the power amplifier with a dc output voltage of 0–10 V. The motor of the Quanser rotary servo unit allows −6 to 6 V range dc input, according to its user manual. Therefore, the system input u is constrained within 0–6 V, i.e., $u_{\min} = 0$ V and $u_{\max} = 6$ V. The nominal values of the system parameters are shown in Table II. However, there is no current sensor to measure current i in this

TABLE III
CONTROL PARAMETERS

Parameters	Values	Parameters	Values
$a_m\ b_m$	25	k_1	1000
$a_m + k$	100	k_2	20000
$G_f(s)$	$\frac{a_0}{s+a_0}$	u_{min}	0 V
a_0	200	u_{max}	6 V

system. This second-order system (30) and (31) can be further reduced to a first-order system to facilitate the control design

$$\dot{\omega} = -\left(\frac{b}{J_m} + \frac{k_t k_\omega}{J_m R_m}\right)\omega + \frac{k_t}{J_m R_m}u + u_d \qquad (32)$$

where $u_d = -\frac{k_t L_m}{J_m R_m}\dot{i} - \frac{T_l}{J_m}$ represents the lumped uncertainty and disturbance term. The reference model of the speed command is selected as $\dot{\omega}_m = -a_m\omega_m + b_m c$. And the error dynamics is defined as $\dot{e}_\omega = -k_0(t)(a_m + k)e_\omega$, where $e_\omega = \omega_m - \omega$ is the tracking error. Apparently, the structural constraint (21) is met in this system. The control parameters are shown in Table III.

A. Case I: Comparison With the Conventional UDE-Based Controller Plus a Saturation Unit and the BIC

In this case, the proposed bounded UDE-based controller (10)–(12) is compared with both the conventional UDE-based controller (6) in [1] plus a saturation unit and the BIC in [19]. For clarity, the output of the conventional UDE-based controller (6) is defined as u_o, and the final controller output after the saturation unit is defined as u to keep consistent variables with the proposed bounded UDE-based controller. The conventional UDE-based controller has the same control parameters in Table III. The integral gain for BIC is selected as $k_I = 0.5$. The desired speed trajectory is selected as $c = 2000$ r/min for $t \in [0,\ 0.5)$s, $c = 4000$ r/min for $t \in [0.5,\ 1)$ s and $c = 2500$ r/min for $t \in [1, 2]$ s. At $t = 1.5$ s, the load switch is turned OFF to change the resistor load of the generator from 1 Ω to 2 Ω.

The experimental results are shown in Fig. 6. Before $t = 0.5$ s, the proposed bounded UDE-based controller achieves good reference tracking when the controller output is not constrained. When the reference is changed at $t = 0.5$ s, the reference tracking cannot be achieved because of input constraint, as shown in Fig. 6(a), and the final controller output u satisfies the input constraint. Though the newly modified UDE-based controller output u_n has some overshoots, it stops increasing and converges to steady state, due to $k_0 \to 0$, which naturally avoids the integral windup. So, after $t = 1$ s, the bounded UDE-based controller still can achieve reference tracking immediately without the effect of integral windup. The proposed bounded UDE-based controller can reject the disturbances caused by load change at $t = 1.5$ s, because of its robustness. At $t = 0.5$ s, though the conventional UDE-based controller plus a saturation unit can guarantee the input constraint with the saturation unit, the original UDE-based controller output u_o continues increasing due to both nonzero tracking error and integral action in $\frac{1}{1-G_f(s)}$, as shown in Fig. 6(b). So, it cannot achieve reference tracking till $t = 1.4$ s, because of the integral windup. The BIC has some overshoots

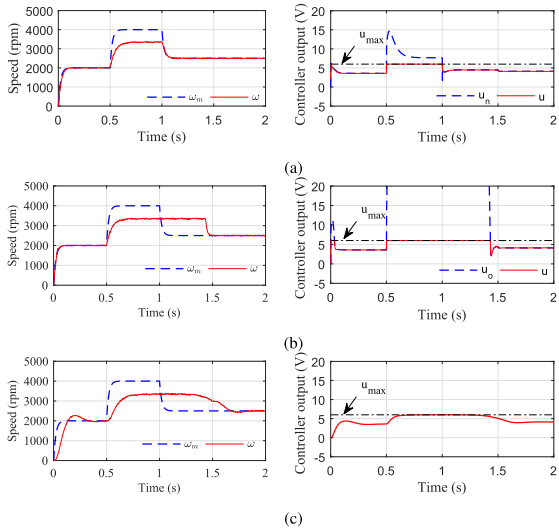

Fig. 6. Case I. Motor speed control results of three control methods with motor speed (left column) and controller output (right column): (a) Proposed bounded UDE-based controller, (b) Conventional UDE-based controller [1] plus a saturation unit, (c) BIC [19].

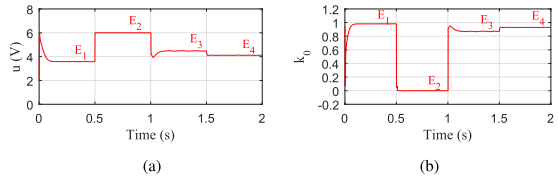

Fig. 7. Case I. The controller states u and k_0 of the proposed bounded UDE-based controller. (a) The final controller output u. (b) The additional variable k_0.

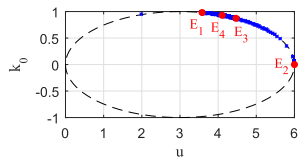

Fig. 8. Case I. The illustration of the controller states u and k_0 on the ellipse.

in reference tracking before $t = 0.5$ s, as shown in Fig. 6(c), and demonstrates the slow responses before $t = 1.7$ s. Though it guarantees the input constraint well, its performances are usually limited by the integral control. Therefore, the proposed bounded UDE-based controller can handle the input constraint without the integral windup, and demonstrates better performances than the conventional UDE-based controller plus a saturation unit and the BIC. The controller states of the proposed bounded UDE-based controller u and k_0 always remain on the ellipse, as illustrated in Figs. 7 and 8, where the controller states converge to the small neighborhoods of the equilibrium points E_1, E_2, E_3, and E_4 at steady states within the periods of 0.3–0.5, 0.8–1, 1.3–1.5, and 1.8–2 s, respectively.

B. Case II: Effects of the Design Parameters

In this case, two sets of design parameters $a_m + k$ and k_2 in the proposed bounded UDE-based controller are investigated,

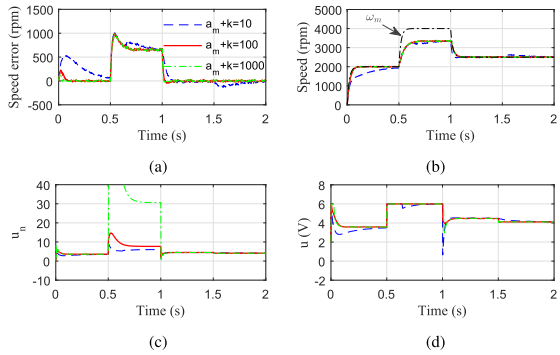

Fig. 9. Case II. Investigation of error feedback gain $a_m + k$. (a) Speed tracking error. (b) Motor speed. (c) The modified UDE-based controller u_n. (d) The final controller output u.

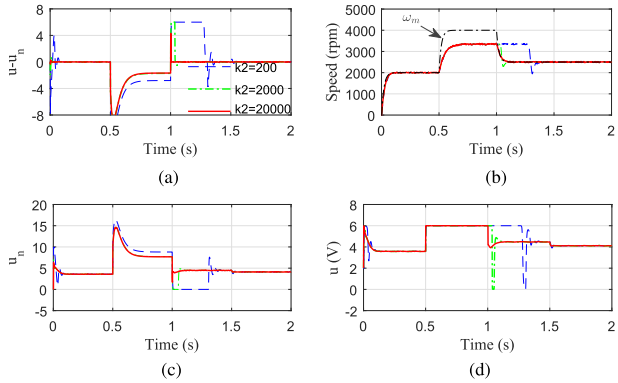

Fig. 10. Case II. Investigation of parameter k_2. (a) $u - u_n$. (b) Motor speed. (c) The modified UDE-based controller u_n. (d) The final controller output u.

and the same experimental procedures of Case I are conducted. Except the investigated parameters, the rest of control parameters are the same as those in Table III.

First, three values of the error feedback gain $a_m + k$ with 10, 100, and 1000 are studied, and the corresponding system responses are shown in Fig. 9. Basically, the larger $a_m + k$ is selected, the better performances of both reference tracking and disturbance rejection can be achieved except for the time periods of 0.5–1 s, due to the input constraint, as shown in Fig. 9(a) and (b). If $a_m + k$ is selected too small, e.g., $a_m + k = 10$, the system has slow response for both reference tracking and disturbances rejection. However, if the $a_m + k$ is selected too large, e.g., $a_m + k = 1000$, though the motor speed regulation can be guaranteed, the larger control efforts are required in both the newly modified UDE-based controller u_n, and the final controller output u, as illustrated in Fig. 9(c) and (d). Therefore, the parameter $a_m + k$ determines the converging rate of the tracking performances, as discussed in Section III-D.

Furthermore, three values of k_2 with 200, 2000, and 20000 are studied, and the experimental results are shown in Fig. 10. The larger k_2 is selected, the faster convergence from the final controller output u to the newly modified UDE-based controller u_n is achieved, except the period with the input constraint, as shown in Fig. 10(a). The better performances of both reference

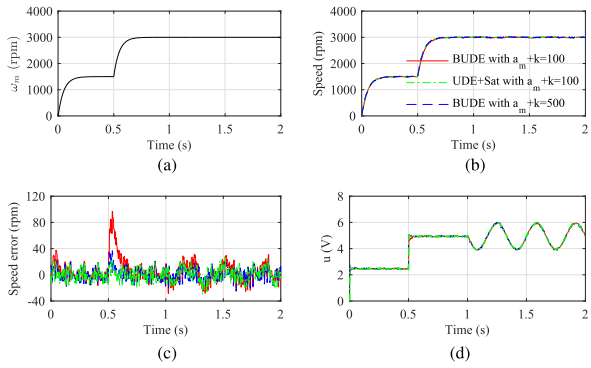

Fig. 11. Case III. Performance investigation when the controller output does not reach the bounds (BUDE: bounded UDE-based control, UDE+Sat: conventional UDE-based control plus a saturation unit). (a) Speed reference. (b) Motor speed. (c) The speed tracking error. (d) The final controller output u.

tracking and disturbance rejection are achieved, as illustrated in Fig. 10(b). Therefore, k_2 determines the converging rate from u to u_n, as discussed in Section III-A. If k_2 is chosen too small, e.g., $k_2 = 200$, the final controller output u cannot track the newly modified UDE-based controller u_n quickly, then the system even could not timely handle the integral windup issue. Therefore, k_2 plays an important role in the proposed bounded control design to effectively deal with input constraint without integral windup.

C. Case III: Performance Investigation When the Controller Output Does Not Reach the Bounds

In this case, the proposed bounded UDE-based controller is investigated when the controller output does not reach the bounds to demonstrate that the proposed control strategy can perform similarly as the conventional UDE control strategy. The desired speed trajectory is selected as $c = 1500$ r/min for $t \in [0,\ 0.5)$s, and $c = 3000$ r/min for $t \in [0.5,\ 2]$s. At $t = 1$ s, a sinusoidal input disturbance with $d(t) = 1.256 \times 10^3 \sin(6\pi t)$ is added into u_d in system (32). The proposed bounded UDE-based controller and the conventional UDE-based controller (6) are compared with the same parameters, where $a_m + k = 100$, and the filter is designed with the combination of a first-order low-pass filter and a second-order bandpass filter $G_f(s) = 1 - (1 - \frac{200}{s+200}) \cdot (1 - \frac{0.6\pi s}{s^2+0.6\pi s+(6\pi)^2})$ to handle the sinusoidal disturbance based on the IMP. In order to further improve the performance of the proposed controller, the large value of $a_m + k$ with $a_m + k = 500$ is investigated. The rest of control parameters are shown in Table III.

The experimental results are shown in Fig. 11. Before $t = 1$ s, both the bounded UDE-based controller and the conventional UDE-based controller plus a saturation unit can achieve reference tracking as shown in Fig. 11(b). The speed tracking error is shown in Fig. 11(c), and some noises can be noticed in the speed measurement. The noises are caused by many reasons, such as gear vibration or encoder sensor deviation. The most important reason is that the measurement noise is amplified by 70 times because of the gear ratio according to user manual, where the encoder sensor is placed at low-speed shaft, and

TABLE IV
RMS VALUE OF THE SPEED TRACKING ERROR (1–2 S)

Controllers	BUDE with $a_m + k = 100$	UDE+SAT with $a_m + k = 100$	BUDE with $a_m + k = 500$
RMS error (rpm)	13.4	10.6	9.5

the system model (32) is obtained from the high-speed shaft side. Compared with the conventional UDE-based controller, the bounded UDE-based controller with same $a_m + k$ has larger tracking errors during the transient stages; however, both of them have similar steady-state tracking performance, as shown in Fig. 11(c). After $t = 1$ s, both controllers can handle the sinusoidal disturbance with the filter design based on the IMP. However, the bounded UDE-based controller with $a_m + k = 100$ has larger tracking errors, as shown in Fig. 11(c) and Table IV, because of the effect from the decrease of k_0. The root-mean-square (RMS) value of the speed tracking error during 1–2 s with the bounded UDE-based controller is 13.4 r/min, while the conventional UDE-based controller is 10.6 r/min. When a large value of $a_m + k = 500$ is adopted in the bounded UDE-based controller, the transient performance is improved significantly with a smaller speed tracking error before $t = 1$ s. The RMS value of the speed tracking error during 1–2 s is reduced to 9.5 r/min. Therefore, the effect from the decrease of k_0 can be mitigated with a proper design of $(A_m + K)$ in the controller.

V. CONCLUSION

In this article, a boundedness design was embedded into the conventional UDE-based controller to handle input constraints. In order to avoid integral windup, an additional time-varying variable was introduced into the error dynamics. In addition, a dynamic controller with boundedness design was developed to ensure that the final controller output and the additional time-varying variable always move and remain on an ellipse. The input constraint was naturally fulfilled and the integral windup was avoided with the time-varying variable approaching zero. The proposed controller had a clear structure with guidelines provided for parameter selections. Both theoretical analysis and experimental results have demonstrated the effectiveness of the approach.

In this article, only single-input systems are considered. For the systems with multiple inputs, the problem is more challenging, and further investigations need to be conducted. Another problem that is worth investigation is the performance degradation caused by the additional time-varying variable.

APPENDIX
GUIDELINES FOR CONTROLLER IMPLEMENTATION

In practice, (11) and (12) can be simplified with some additional variables. For example, they can be revised as $\dot{u} = \gamma$, $\dot{k}_0 = \delta$, where $\gamma = -k_1\alpha\beta - k_2 k_0^2(u - u_n)$ and $\delta = -k_1 k_0 \beta + \frac{4k_2}{(u_{\max}-u_{\min})^2}\alpha k_0(u - u_n)$ with $\alpha = u - \frac{u_{\max}+u_{\min}}{2}$ and $\beta = \frac{4}{(u_{\max}-u_{\min})^2}\alpha^2 + k_0^2 - 1$. This implementation only includes six variables and two integral actions with some basic addition/subtraction/multiplication operations, which does not need much computational resources. In addition, $\frac{4}{(u_{\max}-u_{\min})^2}$ is a known constant, and the whole bounded UDE-based controller does not include any division operations. Indeed, the whole controller was implemented with a 20-kHz sampling frequency in the experiments of this article. Furthermore, a small positive low-bound ε can be set for k_0 to avoid it from reaching 0.

REFERENCES

[1] Q.-C. Zhong and D. Rees, "Control of uncertain LTI systems based on an uncertainty and disturbance estimator," *ASME Trans. J. Dyn. Syst. Meas. Control*, vol. 126, no. 4, pp. 905–910, Dec. 2004.

[2] K. Youcef-Toumi and O. Ito, "A time delay controller for systems with unknown dynamics," *ASME Trans. J. Dyn. Syst. Meas. Control*, vol. 112, no. 1, pp. 133–142, Mar. 1990.

[3] B. Ren, Y. Wang, and Q.-C. Zhong, "UDE-based control of variable-speed wind turbine systems," *Int. J. Control*, vol. 90, no. 1, pp. 121–136, 2017.

[4] Y. Wang and B. Ren, "Fault ride-through enhancement for grid-tied PV systems with robust control," *IEEE Trans. Ind. Electron.*, vol. 65, no. 3, pp. 2302–2312, Mar. 2018.

[5] J. Ren, Y. Ye, G. Xu, Q. Zhao, and M. Zhu, "Uncertainty-and-disturbance-estimator-based current control scheme for PMSM drives with a simple parameter tuning algorithm," *IEEE Trans. Power Electron.*, vol. 32, no. 7, pp. 5712–5722, Jul. 2017.

[6] S. Y. Gadelovits, Q. C. Zhong, V. Kadirkamanathan, and A. Kuperman, "UDE-based controller equipped with a multi-band-stop filter to improve the voltage quality of inverters," *IEEE Trans. Ind. Electron.*, vol. 64, no. 9, pp. 7433–7443, Sep. 2017.

[7] Y. Ye and Y. Xiong, "UDE-based current control strategy for LCCL-type grid-tied inverters," *IEEE Trans. Ind. Electron.*, vol. 65, no. 5, pp. 4061–4069, May 2018.

[8] R. Sanz, P. Garcia, Q. C. Zhong, and P. Albertos, "Predictor-based control of a class of time-delay systems and its application to quadrotors," *IEEE Trans. Ind. Electron.*, vol. 64, no. 1, pp. 459–469, Jan. 2017.

[9] S. Su and Y. Lin, "Robust output tracking control of a class of non-minimum phase systems and application to VTOL aircraft," *Int. J. Control*, vol. 84, no. 11, pp. 1858–1872, 2011.

[10] J. P. Kolhe, M. Shaheed, T. S. Chandar, and S. E. Talole, "Robust control of robot manipulators based on uncertainty and disturbance estimation," *Int. J. Robust Nonlinear Control*, vol. 23, no. 1, pp. 104–122, Jan. 2013.

[11] S. E. Talole, T. S. Chandar, and J. P. Kolhe, "Design and experimental validation of UDE based controller-observer structure for robust input-output linearisation," *Int. J. Control*, vol. 84, no. 5, pp. 969–984, 2011.

[12] S. E. Talole and S. B. Phadke, "Model following sliding mode control based on uncertainty and disturbance estimator," *ASME Trans. J. Dyn. Syst. Meas. Control*, vol. 130, pp. 1–5, 2008.

[13] Q.-C. Zhong, A. Kuperman, and R. Stobart, "Design of UDE-based controllers from their two-degree-of-freedom nature," *Int. J. Robust Nonlinear Control*, vol. 21, pp. 1994–2008, Nov. 2011.

[14] L. Sun, D. Li, Q. C. Zhong, and K. Y. Lee, "Control of a class of industrial processes with time delay based on a modified uncertainty and disturbance estimator," *IEEE Trans. Ind. Electron.*, vol. 63, no. 11, pp. 7018–7028, Nov. 2016.

[15] B. Ren, Q.-C. Zhong, and J. Dai, "Asymptotic reference tracking and disturbance rejection of UDE-based robust control," *IEEE Trans. Ind. Electron.*, vol. 64, no. 4, pp. 3166–3176, Apr. 2017.

[16] I. Aharon, D. Shmilovitz, and A. Kuperman, "Uncertainty and disturbance estimator-based controllers design under finite control bandwidth constraint," *IEEE Trans. Ind. Electron.*, vol. 65, no. 2, pp. 1439–1449, Feb. 2018.

[17] I. Aharon, D. Shmilovitz, and A. Kuperman, "Phase margin oriented design and analysis of UDE-based controllers under actuator constraints," *IEEE Trans. Ind. Electron.*, vol. 65, no. 10, pp. 8133–8141, Oct. 2018.

[18] C. Bohn and D. P. Atherton, "An analysis package comparing PID anti-windup strategies," *IEEE Control Syst. Mag.*, vol. 15, no. 2, pp. 34–40, Apr. 1995.

[19] G. C. Konstantopoulos, Q.-C. Zhong, B. Ren, and M. Krstic, "Bounded integral control of input-to-state practically stable nonlinear systems to guarantee closed-loop stability," *IEEE Trans. Automat. Control*, vol. 61, no. 12, pp. 4196–4202, Dec. 2016.

[20] S. Tarbouriech and M. Turner, "Anti-windup design: An overview of some recent advances and open problems," *IET Control Theory Appl.*, vol. 3, no. 1, pp. 1–19, Jan. 2009.

[21] H. Gao, X. Yang, and P. Shi, "Multi-objective robust H_∞ control of spacecraft rendezvous," *IEEE Trans. Control Syst. Technol.*, vol. 17, no. 4, pp. 794–802, Jul. 2009.
[22] T. Tarczewski and L. M. Grzesiak, "Constrained state feedback speed control of PMSM based on model predictive approach," *IEEE Trans. Ind. Electron.*, vol. 63, no. 6, pp. 3867–3875, Jun. 2016.
[23] K. Esfandiari, F. Abdollahi, and H. A. Talebi, "Adaptive control of uncertain nonaffine nonlinear systems with input saturation using neural networks," *IEEE Trans. Neural Netw. Learn. Syst.*, vol. 26, no. 10, pp. 2311–2322, Oct. 2015.
[24] Y. Wang, B. Ren, and Q.-C. Zhong, "Bounded UDE-based controller for systems with input constraints," in *Proc. 57th IEEE Conf. Decis. Control*, 2018, pp. 2976–2981.
[25] B. A. Francis and W. M. Wonham, "The internal model principle of control theory," *Automatica*, vol. 12, no. 5, pp. 457–465, Sep. 1976.
[26] Y. Wang, B. Ren, and Q.-C. Zhong, "Robust power flow control of grid-connected inverters," *IEEE Trans. Ind. Electron.*, vol. 63, no. 11, pp. 6887–6897, Nov. 2016.
[27] Q.-C. Zhong, Y. Wang, and B. Ren, "UDE-based robust droop control of inverters in parallel operation," *IEEE Trans. Ind. Electron.*, vol. 64, no. 9, pp. 7552–7562, Sep. 2017.
[28] Y. Eun, J.-H. Kim, K. Kim, and D.-I. D. Cho, "Discrete-time variable structure controller with a decoupled disturbance compensator and its application to a CNC servomechanism," *IEEE Trans. Control Syst. Technol.*, vol. 7, no. 4, pp. 414–423, Jul. 1999.
[29] Y. Eun and D.-I. D. Cho, "Robustness of multivariable discrete-time variable structure control," *Int. J. Control*, vol. 72, no. 12, pp. 1106–1115, 1999.
[30] J.-S. Han, T.-I. Kim, T.-H. Oh, S.-H. Lee, and D.-I. D. Cho, "Effective disturbance compensation method under control saturation in discrete-time sliding mode control," *IEEE Trans. Ind. Electron.*, 2019, to be published, doi: 10.1109/TIE.2019.2931213.
[31] Z.-P. Jiang, A. R. Teel, and L. Praly, "Small-gain theorem for ISS systems and applications," *Math. Control Signals Syst.*, vol. 7, no. 2, pp. 95–120, Jun. 1994.
[32] H. K. Khalil, *Nonlinear Systems*. Upper Saddle River, NJ, USA: Prentice-Hall, 2001.

Yeqin Wang (Member, IEEE) received the B.Eng. degree in automotive engineering from the China Agricultural University, China, in 2009, the M.Eng. degree in automotive engineering from the Clean Energy Automotive Engineering Center, Tongji University, China, in 2012, and the Ph.D. degree in Wind Science & Engineering from the National Wind Institute, Texas Tech University, USA, in 2019.

He is currently the Director of Technology with SYNDEM LLC, Chicago, IL, USA. His research interests include robust control, power electronics control, renewable energy, and microgrids.

Beibei Ren (Senior Member, IEEE) received the B.Eng. degree in mechanical & electronic engineering and the M.Eng. degree in automation from the Xidian University, Xi'an, China, in 2001 and 2004, respectively, and the Ph.D. degree in the electrical and computer engineering from the National University of Singapore, Singapore, in 2010.

From 2010 to 2013, she was a Postdoctoral Scholar at the Department of Mechanical & Aerospace Engineering, University of California, San Diego, CA, USA. She is currently an Associate Professor with the Department of Mechanical Engineering, Texas Tech University, Lubbock, TX, USA. Her research interests include robust control, power electronics control, microgrids, and smart grid.

Dr. Ren received the TechConnect National Innovation Award for her microgrid control technology. She serves as Associate Editor for IEEE TRANSACTIONS ON INDUSTRIAL ELECTRONICS and IEEE ACCESS.

Qing-Chang Zhong (Fellow, IEEE) received the Ph.D. degree in control and power engineering from the Imperial College London, UK, in 2004, and the Ph.D. degree in control theory and engineering from the Shanghai Jiao Tong University, Shanghai, China, in 2000.

He is the Founder and Chief Executive Officer of Syndem LLC, Chicago, IL, USA. He is/was a Distinguished Lecturer of IEEE Power Electronics Society, IEEE Control Systems Society, and IEEE Power and Energy Society, and the Vice-Chair of IFAC TC Power and Energy Systems. He was a Senior Research Fellow of Royal Academy of Engineering, UK, and the UK Representative to European Control Association. He holds the Max McGraw Endowed Chair Professor in Energy and Power Engineering with the Department of Electrical and Computer Engineering, Illinois Institute of Technology, Chicago, IL, USA. He is the (co-)author of four research monographs. His research interests include power electronics and advanced control systems theory, together with their seamless integration to address fundamental challenges in power and energy systems.

Dr. Zhong served as the Associate Editor for IEEE TRANSACTIONS ON AUTOMATIC CONTROL, IEEE TRANSACTIONS ON INDUSTRIAL ELECTRONICS, IEEE TRANSACTIONS ON POWER ELECTRONICS, IEEE TRANSACTIONS ON CONTROL SYSTEMS TECHNOLOGY, IEEE ACCESS, and IEEE JOURNAL OF EMERGING AND SELECTED TOPICS IN POWER ELECTRONICS. He is a Fellow of IET. He proposed the SYNDEM (meaning synchronized and democratized) grid architecture for the next-generation smart grid to unify the interaction of power system players with the grid for autonomous operation through the synchronization mechanism of synchronous machines, without relying on communication network.